tvst

Article

# Thickness of the Protective Layers of Different Ophthalmic Viscosurgical Devices During Lens Surgery in a Porcine Model

**Melanie Wüst[1,*], Philipp Matten[2,*], Magdalena Nenning[3], and Oliver Findl[3]**

[1] Faculty of Optics and Mechatronics, University of Aalen, Aalen, Germany
[2] Center for Medical Physics and Biomedical Engineering, Medical University of Vienna, Vienna, Austria
[3] VIROS – Vienna Institute for Research in Ocular Surgery, A Karl Landsteiner Institute, Hanusch Hospital, Vienna, Austria

**Correspondence:** Oliver Findl, Hanusch Hospital, Department of Ophthalmology, Heinrich-Collin-Straße 30, 1140 Vienna, Austria.
e-mail: oliver@findl.at

**Received:** August 2, 2021
**Accepted:** January 20, 2022
**Published:** February 17, 2022

**Keywords:** thickness determination; OVDs; protective layer; optical coherence tomography; segmentation

**Citation:** Wüst M, Matten P, Nenning M, Findl O. Thickness of the protective layers of different ophthalmic viscosurgical devices during lens surgery in a porcine model. Transl Vis Sci Technol. 2022;11(2):28, https://doi.org/10.1167/tvst.11.2.28

**Purpose:** To evaluate the thickness of the intraoperative layers of 10 different ophthalmic viscosurgical devices (OVD) covering the corneal endothelium during simulated lens surgery in a porcine model.

**Methods:** This experimental study took place at the Center for Medical Physics and Biomedical Engineering, Medical University of Vienna, Austria. Ten OVDs with different viscoelastic properties (ProVisc, Z-Hyalin plus, Amvisc plus, DisCoVisc, Healon EndoCoat, Viscoat, Z-Hyalcoat, Combivisc, Duo-Visc, and Twinvisc) were assessed in 10 porcine eyes each, yielding a total of 100 eyes. Simulated cataract surgery was performed with volumetric intraoperative OCT imaging during phacoemulsification and during irrigation/aspiration to determine the remaining amount of OVD coating the endothelium over a scan field of 6 × 6 mm. Indirect visualization of the OVD was enabled by replacing the irrigating solution by a higher scattering diluted milk solution. A deep convolutional neural network (CNN) was used to evaluate OVD layer thickness based on the B-scans.

**Results:** Median thickness values after phacoemulsification were lowest for the cohesive OVDs Z-Hyalin plus (38 µm) and ProVisc (39 µm), followed by the combination systems Twinvisc (342 µm) and Duo-Visc (537 µm). Highest values were observed for the dispersive OVDs and the combination system Combivisc (Viscoat: 957 µm; Z-Hyalcoat: 988 µm, Combivisc: 1042 µm; Amvisc plus: 1259 µm; Healon EndoCoat: 1303 µm; DisCoVisc: 1356 µm). The difference between the OVDs was statistically significant ($P < 0.01$).

**Conclusions:** The results of this study confirm that at completion of phacoemulsification, thickest residual layers of OVD remain when using dispersive substances, followed by combination systems and lowest thickness values were observed with cohesive OVDs. The use of an intraoperative OCT and a deep convolutional neural network allowed measurements over a large scan field of 6 × 6 mm and a precise evaluation of the OVD layer coating the corneal endothelium. The OVD layer seemed to be more like a ragged terrain instead of a flat layer, indicating that the film-forming effect of dispersive OVDs is the result of their volume rheology rather than a surface interaction.

**Translational Relevance:** Evaluating the protective properties provides valuable insights into how different OVDs with different viscoelastic properties form layers beneath the corneal endothelium and helps to understand their persistence during the various steps of cataract surgeries.

## Introduction

Continuing advances in cataract surgery have resulted in improved visual outcomes and safety of the procedure. However, postoperative visual acuity can be compromised by corneal endothelial cell dysfunction and loss, caused by mechanical or biochemical injury during surgery. A decrease in endothelial pump function may lead to corneal edema,

Descemet's membrane folds, and corneal decompensation in patients with low endothelial cell counts.[1]

Ophthalmic viscosurgical devices (OVDs) are widely used during anterior segment surgery to not only facilitate the surgical procedure and maintain space in the anterior chamber, but also to protect the corneal endothelial cells.[1] Depending on their rheological properties, OVDs are usually classified as dispersive or cohesive materials, which both bear advantages and disadvantages.

Cohesive OVDs help to maintain the volume of the anterior chamber and thereby its structural integrity. They are easily removed toward the end of surgery. However, they are prone to flowing out of the eye during phacoemulsification and are thought to offer low protection to the corneal endothelial cells. Because dispersive OVDs tend to adhere to intraocular structures and instruments, they are thought to be more effective in coating the corneal endothelium and, therefore, providing a greater level of protection. However, they are less effective at maintaining adequate space and are sometimes difficult to be completely removed from the anterior chamber.[2,3]

Viscoadaptive OVDs act as cohesive agents at low flow rates; they are highly retentive for maintaining space during surgical manipulation. At high flow rates, they act as pseudodispersive agents by coating the endothelium and also being difficult to fully aspirate.

More recently developed viscous-dispersive OVDs combine the properties of both lower viscosity and higher viscosity materials owing to their intermediate cohesive/dispersive index.[4] In a commonly used method known as the soft shell technique, dispersive and cohesive OVDs are used together in sequence to maximize the advantages and minimize the disadvantages of both groups.[5]

The aim of this study was to compare 10 different OVDs in terms of their endothelial coating properties during cataract surgery as simulated in a porcine eye model.

# Methods

## Porcine Eyes

Porcine eyes derived from pigs slaughtered 1 day before the experiment at the age of 4 months, were purchased from a local abattoir. Because porcine eyes are available commercially, ethics approval was not required.

## OVDs

We assessed 10 different commercially available OVDs:

- Two cohesive OVDs: ProVisc (Alcon, Fort Worth, TX), Z-Hyalin plus (Carl Zeiss Meditec AG, Jena, Germany)
- Five dispersive OVDs: Amvisc plus (Bausch & Lomb, Laval, Canada), DisCoVisc (Alcon), Healon EndoCoat (Johnson & Johnson, New Brunswick, NJ), Viscoat (Alcon), Z-Hyalcoat (Carl Zeiss Meditec AG)
- And three combination systems: Combivisc (Carl Zeiss Meditec AG), Duo-Visc (Alcon) and Twinvisc (Carl Zeiss Meditec AG).

The specific characteristics of these OVD are shown in Table 1.

## Simulated Cataract Surgery

Each eye was mounted to perform simulated cataract surgery using an operating microscope (OPMI Lumera 700, Carl Zeiss Meditec AG). At first, a self-sealing 2-mm incision was made, followed by injection of OVD and an exposure time of 5 minutes to bridge the time of the paracenteses not required in the experimental procedure and to ensure complete adhesion of the OVD to the corneal endothelium. Then, an anterior continuous curvilinear capsulorhexis was performed. As sculpting, the process of debulking the central nucleus, was not necessary in the young, soft lenses of the porcine eyes, this step was simulated by irrigation/aspiration (I/A) without the use of ultrasound guidance (device settings: vacuum level, 100 mm Hg; aspiration flow rate, 20 mm/min; bottle height, 80 cm $H_2O$; time, 1 min).

Optical coherence tomography (OCT) imaging was used to determine the remaining amount of OVD at this time point (first measurement). A standard 6-mm scan with the RESCAN 700 (Carl Zeiss Meditec AG) was used, Additionally, to visualize the OVD in the anterior chamber, milk was added to the balanced salt solution, which was used during I/A and phacoemulsification, in a mixing ratio of 100:1. Owing to the higher scattering properties of this material, a distinction between the clear OVD and the diluted milk in the OCT image was enabled.

Segment removal of the lens was done by using a phacoemulsification probe (Visalis V500, Zeiss Meditec AG; device settings: vacuum level, 400 mm Hg; aspiration flow rate, 40 mm/min; bottle height, 80 cm $H_2O$; power, 40%; effective phacoemulsification

**Table 1.** Specific Characteristics of the OVDs

| | Composition | Molecular Weight (Daltons) | Viscosity[a] (mPa.s) | CDI (asp%/mm Hg) | Quantity Per Cannula (mL) |
|---|---|---|---|---|---|
| Cohesive OVDs | | | | | |
| ProVisc | 1.0% NaHa | 2,500,000 | 25,000 | 50 | 0.85 |
| Z-Hyalin plus | 1.5% NaHa | 2,900,000 | 295,000 | 44 | 0.85 |
| Dispersive OVDs | | | | | |
| Amvisc Plus | 1.6% NaHa | 1,000,000 | 100,000 | 21.4 | 0.8 |
| DisCoVisc[b] | 1.65% NaHa<br>4.0% CDS | 1,650,000 | 75,000 | 12 | 1.0 |
| Healon EndoCoat | 3.0% NaHa | 800,000 | 50,000 | 3.4 | 0.85 |
| Viscoat | 3.0% NaHa<br>4.0% CDS | 500,000<br>23,000 | 50,000 | 3.4 | 0.5 |
| Z-Hyalcoat | 3.0% NaHa | 1,000,000 | 47,000 | 18 | 0.85 |
| Combination systems | | | | | |
| Combivisc cohesive | | = Z-Hyalin plus | | | 1.0 |
| Combivisc dispersive | | = Z-Hyalcoat | | | 0.85 |
| DuoVisc cohesive | | = ProVisc | | | 0.35 |
| DuoVisc dispersive | | = Viscoat | | | 0.4 |
| Twinvisc cohesive | 1.0% NaHa | 2,100,000 | 18,000 | 36 | 0.7 |
| Twinvisc dispersive | 2.2% NaHa | 1,000,000 | 14,000 | 26 | 0.7 |

[a]Viscosity values reflect manufacturer's information. Viscosity is indicated either as dynamic or zero-shear viscosity. Above values are not directly comparable.

[b]Intermediate cohesive/dispersive index.

time, 7 seconds). Because each lens behaves individually during the process of phacoemulsification and the time required for complete removal varies, an average effective phacoemulsification time of 7 seconds was determined. The aim was not to remove the entire lens, but to standardize the experimental conditions. To evaluate the remaining amount of OVD, an OCT volume scan was taken again after this step (second measurement).

## Image Analysis

The 10 different OVDs were tested in 10 porcine eyes each and OCT imaging was performed before and after lens removal, generating a total of 200 OCT volume scans and 25.600 B-scans, respectively. To automate the segmentation and quantification of the remaining OVD in this large volume database, a deep convolutional neural network, whose architecture is based on the U-Net, as described by Ronneberger et al.,[6] was used to evaluate OVD layer thickness based on the B-scans. Training and validation data, which are required for machine learning, were generated by manual segmentation of more than 3000 B-scans with a 90/10 split between the training and validation data. For this purpose, the contrast of the B-scans was increased, and its noise decreased by means of image filters and the images were scaled to 1024 × 1024 pixels by bicubic interpolation. Marks were set manually at the endothelium–OVD and the OVD–milk solution interfaces to create masks, which served as ground truth for training. The network was applied to each individual B-scan, whereupon the mask was generated automatically and the operator decided whether the result was correct. An accuracy of 99.1% was achieved when applied upon training data. OVD layer thickness was then calculated from the distance between the segmented portions of the images: the corneal endothelium and the hyperreflective milk solution. Figure 1 shows a central anterior chamber cross-section immediately after I/A was completed. After the creation of the mask, the distance between the corneal endothelium and the hyper-reflective milk solution can be quantified as the remaining OVD layer. To demonstrate more explicitly how irregular the shape of the milk solution and hence the OVD layer behaves, a volume rendering was further created. Figure 2 shows an example for the OVD Amvisc plus.

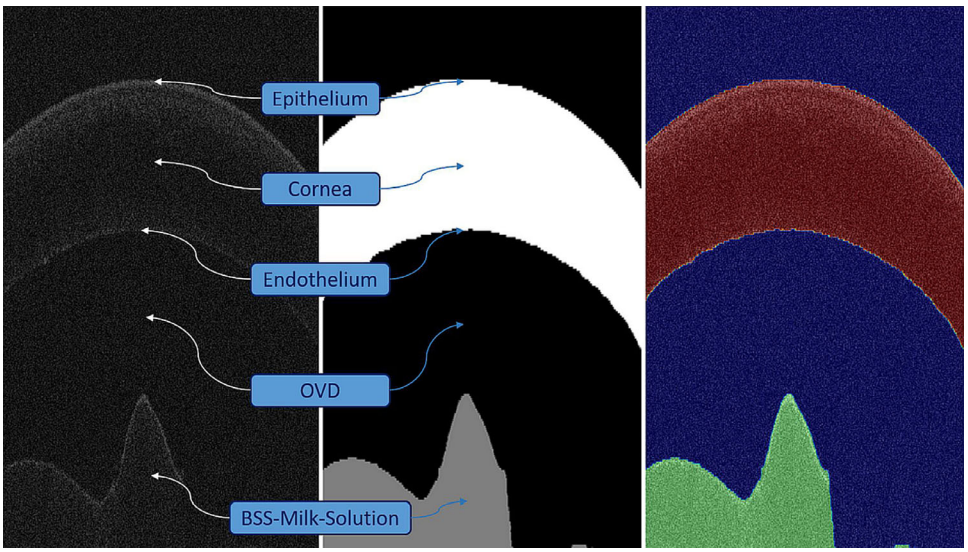


**Figure 1.** OCT image of the anterior chamber after I/A including the creation of a mask to quantify the remaining OVD layer. BSS: balanced salt solution.

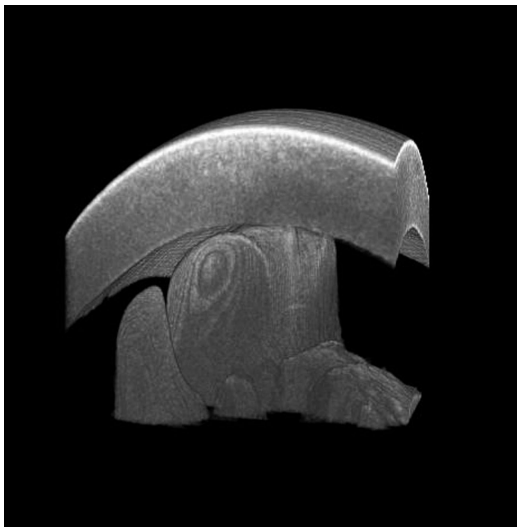

**Figure 2.** Example of a volume rendering of the anterior chamber for Amvisc Plus demonstrating the irregular shape of the OVD/milk solution interface.

**Table 2.** Refractive Indices of the OVDs

| | Refractive Index |
|---|---|
| ProVisc | 1.357 |
| Z-Hyalin plus | 1.364 |
| Amvisc Plus | 1.356 |
| DisCoVisc | 1.337 |
| Healon EndoCoat | 1.357 |
| Viscoat | 1.356 |
| Z-Hyalcoat | 1.343 |
| Combivisc | 1.353 |
| DuoVisc | 1.356 |
| Twinvisc | 1.353 |

## Data Analysis

To compare the results based on the OCT images, the refractive index of each OVD needed to be defined. Therefore, a calibration cuvette of known thickness was used and OCT imaging took place to determine the path length difference between air and each OVD within the walls of the cuvette. For the combination systems, an average refractive index of the OVD mixture present in the anterior chamber at the time of measurement was estimated by using weighted average values of the refractive indices of the two subsets (weighting: 2/3 dispersive OVD, 1/3 cohesive OVD). The measurements were performed in a similar way, however, without monitoring the temperature during the experiment.

The refractive indices of the OVDs, as listed in Table 2 were calculated by Snell's law and used to convert from optical [pixels] to geometric [micrometers] path lengths. Those values were applied to the entire OCT volume scan and plotted as heat maps. When considering the segmentation and image processing error threshold and the resolution of the OCT image, the lateral accuracy of our evaluations was approximately 25 µm.

A data analysis was performed using MATLAB (2019b) and Python (3.7.1) software and, because our data were not normally distributed, the nonparametric Kruskal–Wallis test was used to test for differences

between the groups. A $P$ value of less than .05 was defined as significant.

To further evaluate the results, a threshold of 200 µm was defined as the minimum thickness needed to provide a certain degree of protection to the endothelium. So far, no existing data indicate how thick the remaining OVD layer needs to be for sufficient protection. Thus, we used the information on average values of residual OVD volume available in the literature.

The range for cohesive OVDs is approximately 0 to 300 µm, with mean or median values close to 0 µm.[7–9] For dispersive and viscoadaptive OVDs, a higher distribution of ranges is given: 1 to 650 µm,[7] 100 to 550 µm[8] and 390 to 1120 µm,[9] with mean or median values of greater than 250 µm. Based on these data, a limit between cohesive and dispersive OVDs of about 200 µm was estimated and used in the evaluation of this series of experiments as a threshold value.

Because OVD layer thickness proved to behave quite uneven and thickness values varied significantly within one scan, thickness distribution was further evaluated for the central area of the cornea (3 mm in diameter), which is the most vital part to protect during surgery.

## Results

A high fluctuation and inhomogeneity of thickness values within one scan was observed in this study, as can be seen in Figure 3, which shows an example of a heat map for a combination system. In the two-dimensional heat map, a strong disparity between adjacent measurement points becomes visible as sharp

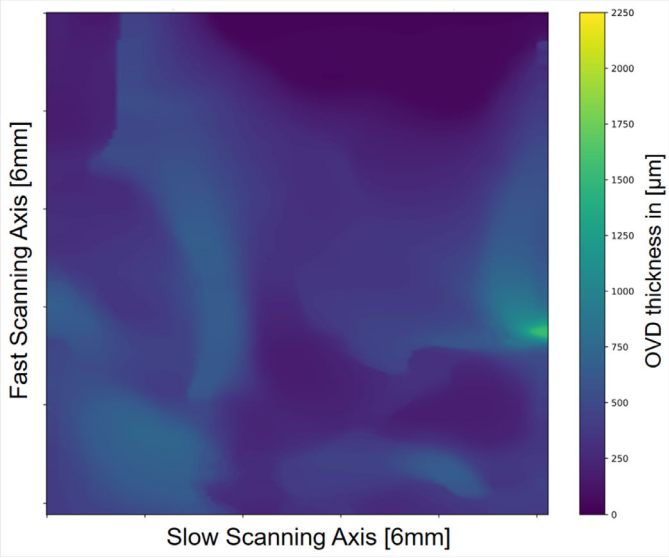


**Figure 3.** Example of OVD thickness distribution for Combivisc displayed as heat map.

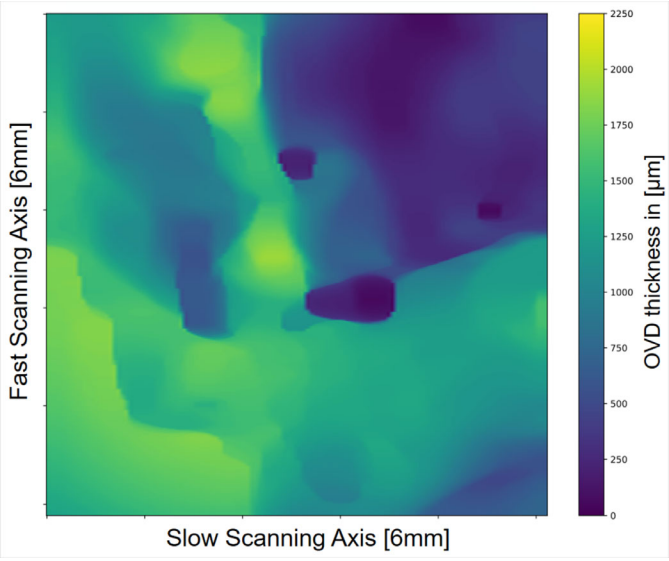


**Figure 4.** Example of OVD thickness distribution for Twinvisc displayed as heat map.

edges in the color display. In the right upper corner, for example, a large dark area represents measured values of less than 500 µm. Next to those minimum values, bright areas that represent maximum thickness values appear without a smooth transition. Small, dark circles appear in the heat maps of all OVDs and may be identified as small air bubbles entrapped within the substances. As a comparison, Figure. 4 shows another example of a heat map for a combination system, with a more even distribution, whereas thickness values are quite low throughout the entire scan.

Thickness values of the first measurement repetition (i.e., after I/A) and the second measurement repetition (i.e., after phacoemulsification) for each OVD varied significantly ($P < 0.01$) and are shown in Table 3. All OVDs showed significantly lower values after phacoemulsification ($P < 0.01$). The violin plots illustrate the variance between the three groups: cohesive OVDs (Fig. 5), dispersive OVDs (Fig. 6), and combination systems (Fig. 7). Violin plots are a combination of box plots and rotated kernel density plots and were used owing to the multimodal distribution of our data. Similar to box plots, the three horizontal lines indicate first quartile, median, and third quartile, respectively; additionally, the full distribution of the data can be read off the smoothed outer shape, which represents all possible results. As can be seen, thickness values show roughly the same distribution within the group of cohesive and the group of dispersive OVDs. When comparing the combination systems among each other, the plots differ in shape much more. The overall slimmer Duo-Visc and Twinvisc plots indicate a higher variance of the results with peaks of less than

**Table 3.** Thickness Values (Median, Minimum and Maximum) of the First (After I/A) and Second (After I/R and Phaco) Measurement Repetition (Whole Map)

| | First MR (After I/A) | | Second MR (After I/R and Phaco) | |
|---|---|---|---|---|
| | Median (µm) | Min/Max (µm) | Median (µm) | Min/Max (µm) |
| ProVisc | 39 | 16/2214 | 39 | 16/2075 |
| Z-Hyalin plus | 1012 | 16/2081 | 38 | 16/1869 |
| Amvisc plus | 1360 | 16/2115 | 1259 | 16/2026 |
| DisCoVisc | 1441 | 17/2236 | 1356 | 17/2157 |
| Healon EndoCoat | 1437 | 16/2058 | 1303 | 16/2024 |
| Viscoat | 1270 | 16/2037 | 957 | 16/2037 |
| Z-Hyalcoat | 1350 | 16/2045 | 988 | 16/2045 |
| Combivisc | 1312 | 16/2086 | 1042 | 16/2098 |
| Duo-Visc | 1057 | 16/2093 | 537 | 16/2003 |
| Twinvisc | 398 | 16/2008 | 342 | 16/1963 |

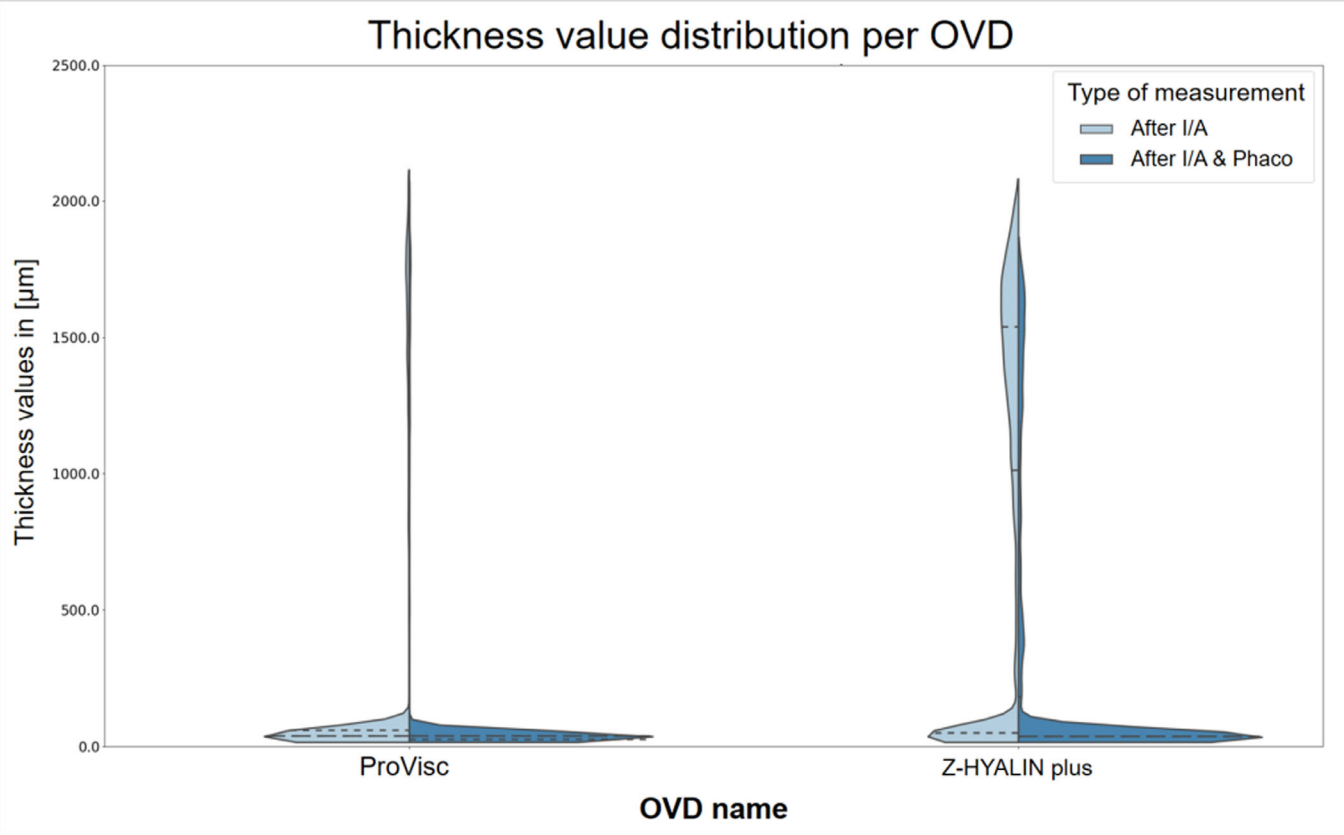


**Figure 5.** Distribution of thickness values: Cohesive OVDs.

1000 µm, whereas the fatter Combivisc plot indicates more evenly distributed values with peaks of less than as well as greater than 1000 µm.

As demonstrated in Figure 3, a high fluctuation of thickness values occurred within one scan, which was overall observed in our study. The most vital part to protect is the very center of the cornea, as a diminished endothelial pump function in this area results in a transient or permanent corneal edema which can seriously compromise postoperative visual acuity. Therefore, in a second step, we analyzed the central 3 mm of the endothelium. The results varied significantly between the different OVDs ($P < 0.01$) and are shown in Table 4.

After the first measurement repetition, the thickness layer in the central 3 mm was thinner for

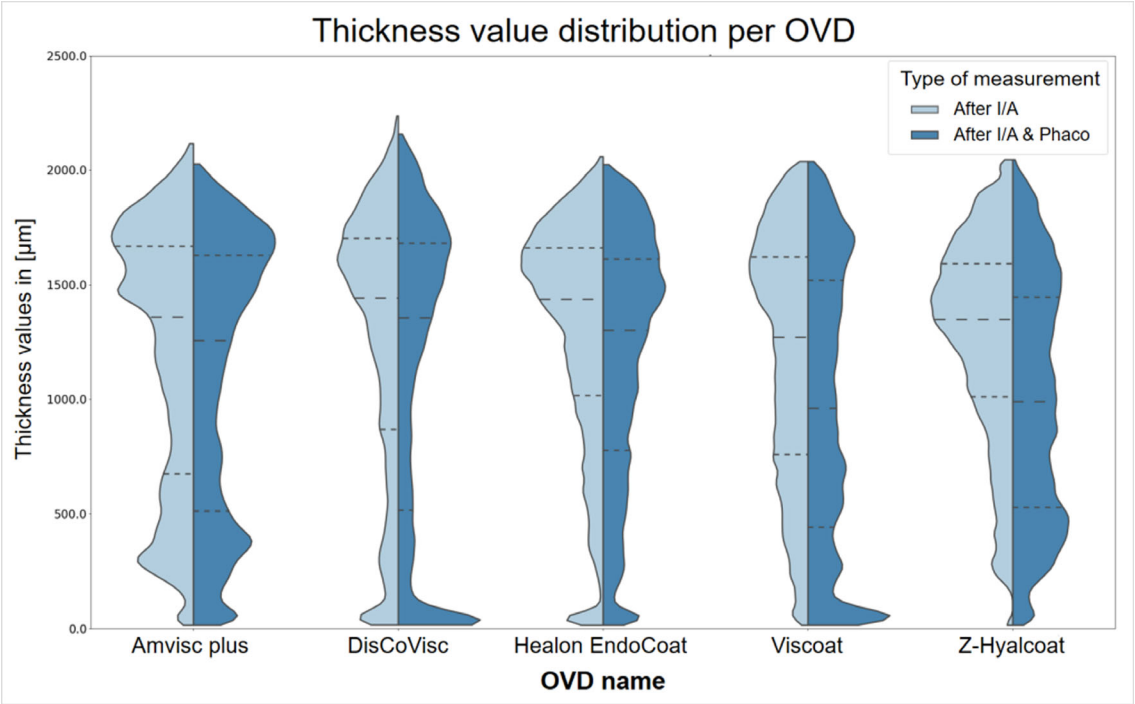


**Figure 6.** Distribution of thickness values: Dispersive OVDs.

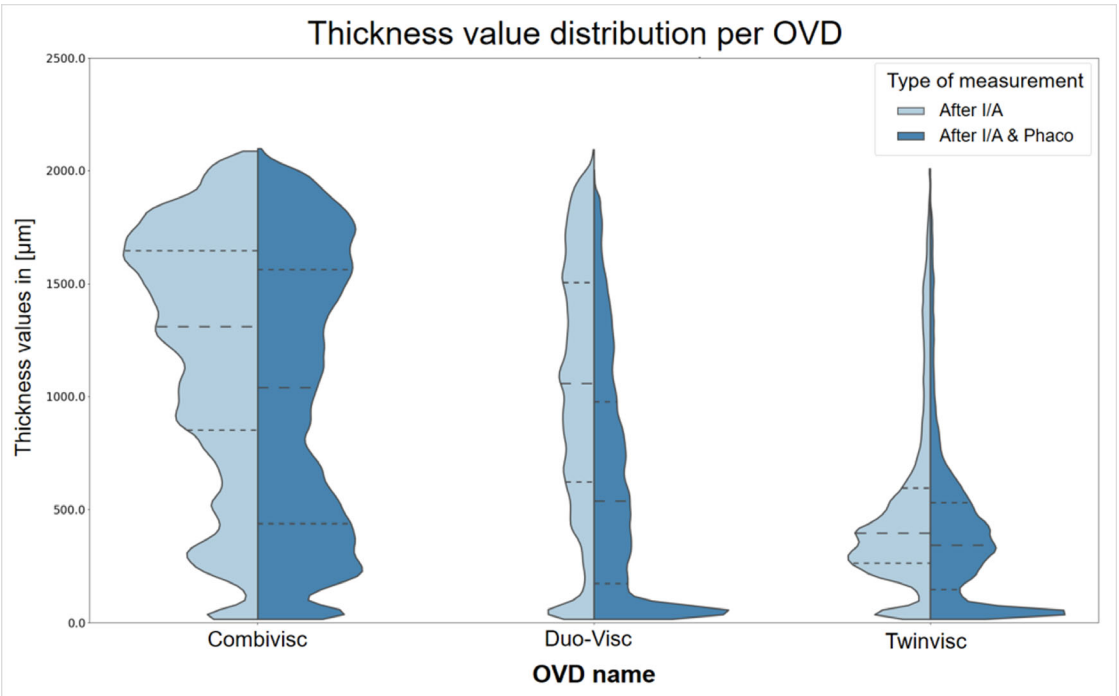


**Figure 7.** Distribution of thickness values: Combination OVD systems.

all OVDs apart from Provisc, Healon EndoCoat, and Twinvisc. After the second measurement repetition, all OVDs showed smaller thickness values in the central 3 mm, when compared with the whole map.

Figure 8 shows a diagram of the percentage of thickness values that exceeded the threshold of 200 µm. When comparing ProVisc and Z-Hyalin plus, considerably higher percentages were observed for the latter, whereas both cohesive OVDs showed lower values than

**Table 4.** Thickness Values (Median, Minimum and Maximum) of the First (After I/A) And second (After I/R and Phaco) Measurement Repetition (Central 3 mm)

| | First MR (After I/A) | | Second MR (After I/R and Phaco) | |
|---|---|---|---|---|
| | Median (µm) | Min/Max (µm) | Median (µm) | Min/Max (µm) |
| ProVisc | 39 | 16/2114 | 27 | 16/2075 |
| Z-Hyalin plus | 829 | 16/2081 | 27 | 16/1858 |
| Amvisc plus | 1018 | 27/2115 | 593 | 16/2015 |
| DisCoVisc | 1424 | 17/2236 | 1135 | 17/2157 |
| Healon EndoCoat | 1549 | 27/2058 | 1264 | 27/2024 |
| Viscoat | 1069 | 16/2037 | 766 | 16/2037 |
| Z-Hyalcoat | 1339 | 28/2045 | 774 | 16/2045 |
| Combivisc | 1116 | 16/2086 | 622 | 16/2098 |
| Duo-Visc | 1024 | 22/2093 | 369 | 16/2003 |
| Twinvisc | 426 | 16/2008 | 319 | 16/1963 |

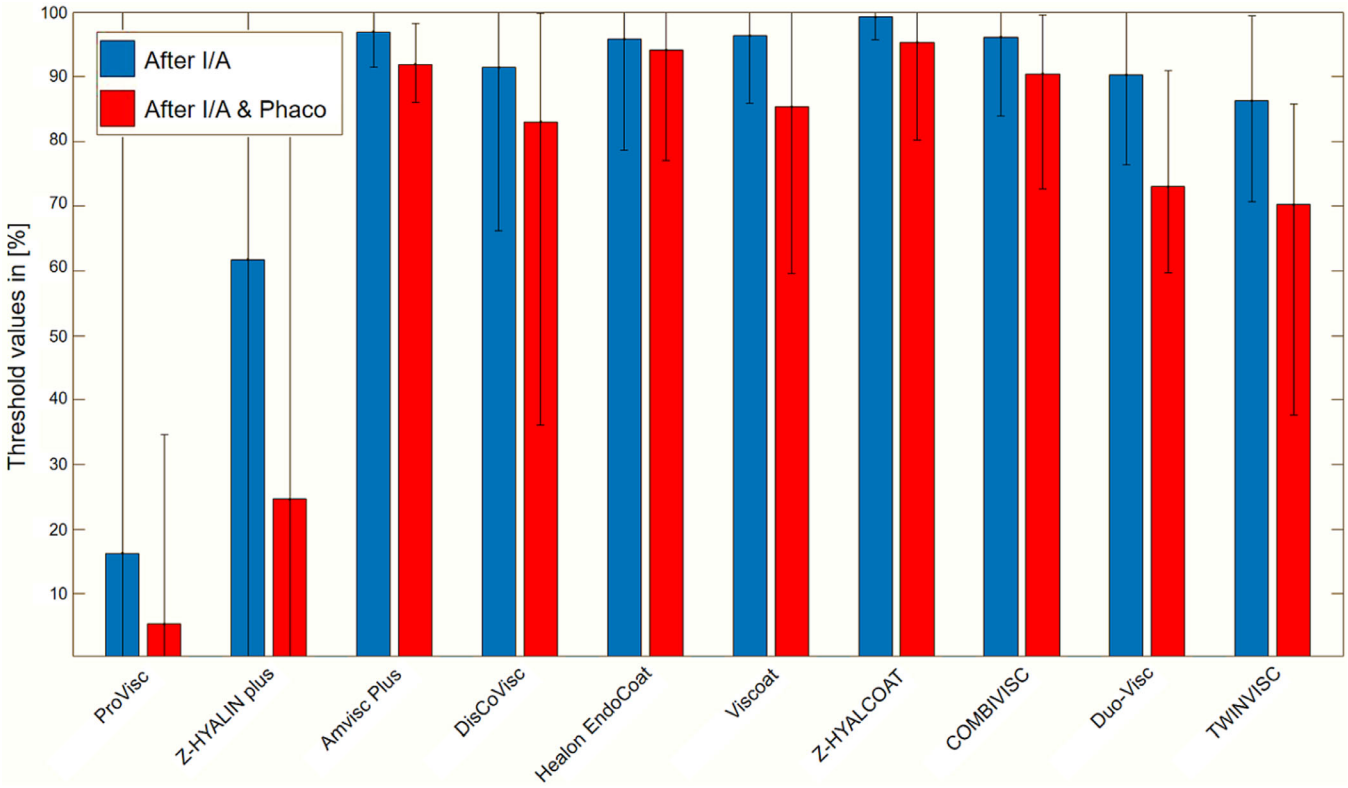


**Figure 8.** Percentage of thickness values exceeding the threshold of 200 µm.

the dispersive OVDs and the combination systems. The highest value was observed for the dispersive Z-Hyalcoat and regarding the combination systems, the percentage of thickness values was highest for Combivisc.

## Discussion

Continuing advances in cataract surgery, such as improved surgical techniques or OVD

materials, involve more specialized OVD formulations with unique rheologic features.[10] Lower viscosity dispersive and higher viscosity cohesive materials both have their advantages and disadvantages, and there is no single ideal substance for all ocular applications. Hence, adequate evaluation of OVD performance is essential to select the best OVD to suit the clinical situation.

In this study, we focused on one important quality of OVDs, namely, their ability to form a protection layer that covers the corneal endothelial cells during cataract surgery, to prevent them from being damaged by mechanical trauma from lens fragments or fluid turbulence during phacoemulsification as well as I/A, all of which would result in a decrease in endothelial pump function.[10,11]

Belda et al.[12] compared OVDs with different concentrations of sodium hyaluronate to a control group in which no OVD was used and showed that all examined OVDs efficiently reduced lesions to the endothelium following oxidative stress induced by $H_2O_2$.

Oshika et al.,[13] in a study similar to ours, investigated the volume of different OVDs in the anterior chamber of porcine eyes after phacoemulsification. However, they only measured the time needed to remove the OVD completely to approximate the residual volume. In the present study, a quantitative method to directly measure the remaining amount of OVD covering the corneal endothelium after phacoemulsification over a large scan field of 6 × 6 mm was evaluated.

The high fluctuation and inhomogeneity of thickness values is consistent with the results of Petroll et al.,[8] Mori et al.,[4] and McDermott et al.,[7] who also observed a high variability in their measurements. A smaller standard deviation of the residual OVD layer thickness was reported by Yoshino et al.,[9] whose images generated by a Scheimpflug camera show more uniform and planar OVD layers compared with the heat maps of our work. However, they did not measure thickness values over a large area of the cornea but rather at one point at its center, which might be the reason for the lower standard deviations.

Some studies state that the presence of chondroitin sulfate as a content of the OVD results in accumulation on the corneal endothelium owing to its large portion of negative charges.[14] By evaluating a large area of the corneal endothelium, the present study showed that the formation of the residual OVD resembles a quite uneven and ragged surface rather than a flat layer, which also applies for the OVDs containing chondroitin sulfate. Hence, the results of this study may indicate the film-forming effect not being a result of the OVD's stickiness or surface interaction but rather it's volume rheology.

Naturally, the amount of residual OVD was significantly lower after phacoemulsification than before phacoemulsification in all tested substances, because the turbulent flow present during phacoemulsification inevitably results in a wash-off of OVD from the anterior chamber.[15]

Increasing device settings during phacoemulsification results in a greater decrease of OVD layer thickness from the first to the second measurement repetition. This decrease is more pronounced for cohesive OVDs, suggesting that cohesive substances are aspirated at lower I/A flow rates.

Many studies have confirmed that cohesive OVDs tend to escape from the anterior chamber as a solid mass during phacoemulsification and, therefore, leave the endothelial cells without sufficient protection,[1,16,17] whereas dispersive OVDs are highly retentive, thus providing good endothelium coverage,[7,10,11,16,18] which is consistent with the results of our study: the largest residual amount of OVD was observed with the dispersive OVDs, followed by the combination systems, whereas Combivisc achieved results similar to those of the dispersive OVDs. The lowest amount of residual OVD was seen with cohesive substances.

When comparing the heat maps of the dispersive OVDs to the combination systems, it becomes apparent that the OVD layers are slightly more homogeneous and uniform when using the latter, whereas the overall thickness values are lower. This finding may be explained by the soft shell technique, which was used when applying the combination systems: the cohesive OVD is injected beneath the dispersive OVD, pushing it toward the cornea and flattening it, which may result in better adhesion to the endothelium. Flattening of the OVD implies a portion of it being displaced toward the periphery; thus, the volume of the dispersive OVD is smaller with the soft shell technique than with the use of a single dispersive OVD, which may account for the overall lower OVD layer thicknesses of the combination systems as opposed to the dispersive OVDs. Future research should analyze the distribution of the two subsets of combination systems in the anterior chamber, for example, by staining the two OVDs with fluorophores fluorescing at different wavelengths. To prevent the small fluorophore molecules from crossing the interface between the OVDs before the two subsets mix up, ideally, OVDs with covalently bound fluorophores should be used. This practice would further be useful for the exact determination of the average refractive index needed to convert from optical (pixels) to geometric (micrometers) path lengths. These

assumptions would need further evaluation, which could be accomplished by using an OCT system with a larger scan field, higher sampling, and isotropic resolution.

The present study has some limitations. First, a porcine model was used. Although the corneal endothelium of pigs resembles the human endothelium by having a similar cell density and shape, the results cannot be applied directly to human eyes. The porcine lenses were young, soft, and easy to extract, whereas in clinical practice, most patients scheduled for cataract surgery present with lenses older and harder, and to be removed, they may consequently require higher ultrasonic energy than the standard device settings used in this study. Second, the extent of endothelial cell damage at the sites of OVD thickness values below the estimated threshold of 200 µm should be evaluated to approve some of the statements arising from this study. Because the refractive index of the OVD depends on temperature and sugar monomer concentration, both of which were not determined during the cuvette measurements to determine the refractive index, there could be some deviations in the exact values of some indices. This error, however, is negligible for the analysis and conclusions carried out in this study.

It would be of interest to analyze whether endothelial cell damage occurs if this threshold is undercut, for example by measuring endothelial cell density.

## What Was Known

- Dispersive OVDs provide a higher level of protection against damage to the corneal endothelium during cataract surgery when compared with cohesive OVDs.[19]

## What This Article Adds

- Using intraoperative OCT and a deep convolutional neural network (U-Net), this study allowed to measure and evaluate OVD layer thickness over a large scan field of 6 × 6 mm.
- The OVD layers were quite uneven and not flat, with thickness values varying significantly within small areas, even when limiting the analysis to the central 3 mm of the cornea. Therefore, visualization over a large area is needed to determine residual OVD volume precisely.
- Combination OVD systems may result in slightly more homogeneous and uniform layer formations when the soft shell technique is applied, whereas the overall thickness values are lower as opposed to the use of a single dispersive OVD.
- Cohesive OVDs result in lower layer thickness than the dispersive and combination OVD systems.

## Acknowledgments

The authors have no proprietary or financial interest in any of the materials or equipment mentioned in this study.

Disclosure: **M. Wüst**, None; **P. Matten**, None; **M. Nenning**, None; **O. Findl**, Alcon (C), Croma (C), Carl Zeiss Meditec AG (C), Johnson & Johnson (C), Merck (C)

[*] MW and PM contributed equally to this work and share the first authorship.

## References

1. Storr-Paulsen A, Nørregaard JC, Farik G, Tårnhøj J. The influence of viscoelastic substances on the corneal endothelial cell population during cataract surgery: a prospective study of cohesive and dispersive viscoelastics. *Acta Ophthalmol Scand*. 2006;85(2):183–187, doi:10.1111/j.1600-0420.2006.00784.x.
2. Auffarth GU, Auerbach FN, Rabsilber T, et al. Comparison of the performance and safety of 2 ophthalmic viscosurgical devices in cataract surgery. *J Cataract Refract Surg*. 2017;43(1):87–94, doi:10.1016/j.jcrs.2016.10.025.
3. Neumayer T, Prinz A, Findl O. Effect of a new cohesive ophthalmic viscosurgical device on corneal protection and intraocular pressure in small-incision cataract surgery: *J Cataract Refract Surg*. 2008;34(8):1362–1366, doi:10.1016/j.jcrs.2008.04.018.
4. Mori H, Yamada H, Toyama K, Takahashi K. A new histological evaluation method to detect residual ophthalmic viscosurgical devices for cataract surgery. *Heliyon*. 2018;4(9):e00822, doi:10.1016/j.heliyon.2018.e00822.
5. Arshinoff SA. Dispersive-cohesive viscoelastic soft shell technique: *J Cataract Refract Surg*. 1999;25(2):167–173, doi:10.1016/S0886-3350(99)80121-7.
6. Ronneberger O, Fischer P, Brox T. U-Net: Convolutional networks for biomedical image segmentation. In: Navab N, Hornegger J,

Wells WM, Frangi AF, eds. *Medical Image Computing and Computer-Assisted Intervention – MICCAI 2015*. Vol. 9351. Lecture Notes in Computer Science. Springer New York: International Publishing; 2015:234–241, doi:10.1007/978-3-319-24574-4_28.

7. McDermott ML, Hazlett LD, Barrett RP, Lambert RJ. Viscoelastic adherence to corneal endothelium following phacoemulsification. *J Cataract Refract Surg*. 1998;24(5):678–683, doi:10.1016/S0886-3350(98)80265-4.
8. Petroll MW, Jafari M, Lane SS, Jester JV, Cavanagh DH. Quantitative assessment of ophthalmic viscosurgical device retention using in vivo confocal microscopy. *J Cataract Refract Surg*. 2005;31(12):2363–2368, doi:10.1016/j.jcrs.2005.05.032.
9. Yoshino M, Bissen-Miyajima H, Ohki S. Residual amounts of ophthalmic viscosurgical devices on the corneal endothelium following phacoemulsification. *Jpn J Ophthalmol*. 2009;53(1):62–64, doi:10.1007/s10384-008-0601-3.
10. Leang RS, Kloft LJ, Gray B, Gwon AE, Huang LC. Preclinical safety evaluation of ophthalmic viscosurgical devices in rabbits and a novel minipig model. *Ophthalmol Ther*. 2019;8(1):101–114, doi:10.1007/s40123-019-0167-9.
11. Higashide. Use of viscoelastic substance in ophthalmic surgery—Focus on sodium hyaluronate. *Clin Ophthalmol*. 2008;2(1):21–30, doi:10.2147/OPTH.S1439.
12. Belda JI, Artola A, García-Manzanares MD, et al. Hyaluronic acid combined with mannitol to improve protection against free-radical endothelial damage: Experimental Model. *J Cataract Refract Surg*. 2005;31(6):1213–1218, doi:10.1016/j.jcrs.2004.11.055.
13. Oshika T. Retention and removal of a new viscous dispersive ophthalmic viscosurgical device during cataract surgery in animal eyes. *Br J Ophthalmol*. 2006;90(4):485–487, doi:10.1136/bjo.2005.085969.
14. Li B, Chen L, Chen Y, et al. The injection of DisCoVisc into the anterior chamber improved corneal preservation and transplantation for cornea blind patients. *Am J Transl Res*. 2017;9(9):4104–4110.
15. Tetz MR, Holzer MP, Lundberg K, Auffarth GU, Burk ROW, Kruse FE. Clinical results of phacoemulsification with the use of Healon5 or Viscoat. *J Cataract Refract Surg*. 2001;27(3):416–420, doi:10.1016/S0886-3350(00)00569-1.
16. Koch DD, Liu JF, Glasser DB, Merin LM, Haft E. A Comparison of corneal endothelial changes after use of Healon or Viscoat during phacoemulsification. *Am J Ophthalmol*. 1993;115(2):188–201, doi:10.1016/S0002-9394(14)73923-6.
17. Miyata K, Maruoka S, Nakahara M, et al. Corneal endothelial cell protection during phacoemulsification: Low- versus high-molecular-weight sodium hyaluronate. *J Cataract Refract Surg*. 2002;28(9):1557–1560, doi:10.1016/S0886-3350(02)01540-7.
18. Poyer JF, Chan KY, Arshinoff SA. New method to measure the retention of viscoelastic agents on a rabbit corneal endothelial cell line after irrigation and aspiration. *J Cataract Refract Surg*. 1998;24(1):84–90, doi:10.1016/S0886-3350(98)80079-5.
19. Peck CMC, Joos ZP, Zaugg BE, et al. Comparison of the corneal endothelial protective effects of Healon-D and Viscoat. *Clin Exp Ophthalmol*. 2009;37(4):397–401, doi:10.1111/j.1442-9071.2009.02034.x.